Dynamic Control System Mode Performance of the Space Technology-7 Disturbance Reduction System

James R. O'Donnell Jr.[ab], Oscar Hsu[a], Peiman Maghami[a]

[a] *Aerospace Engineer, Attitude Control Systems Engineering Branch, NASA Goddard Space Flight Center, Code 591, Greenbelt, Maryland 20771 USA, James.R.ODonnell@nasa.gov*
[b] *Corresponding Author*

Abstract

The Space Technology-7 (ST-7) Disturbance Reduction System (DRS) is an experiment package aboard the European Space Agency (ESA) LISA Pathfinder spacecraft, launched on December 3, 2015. DRS consists of three primary components: Colloidal MicroNewton Thrusters (CMNTs), an Integrated Avionics Unit (IAU), and flight-software implementing the Command and Data Handling (C&DH) and Dynamic Control System (DCS) algorithms. The CMNTs were designed to provide thrust from 5 to 30 μN, with thrust controllability and resolution of 0.1 μN and thrust noise of 0.1 $\mu N/\sqrt{Hz}$ in the measurement band from 1–30 mHz. The IAU hosts the C&DH and DCS flight software, as well as interfaces with both the CMNT electronics and the LISA Pathfinder spacecraft. When in control, the DCS uses star tracker attitude data and capacitive or optically-measured position and attitude information from LISA Pathfinder and the LISA Technology Package (LTP) to control the attitude and position of the spacecraft and the two test masses inside the LTP. After completion of the nominal ESA LISA Pathfinder mission, the DRS experiment was commissioned followed by its nominal mission. DRS operations extended over the next five months, interspersed with stationkeeping, anomaly resolution, and periods where control was handed back to LISA Pathfinder for them to conduct further experiments. The primary DRS mission ended on December 6, 2016, with the experiment meeting all of its Level 1 requirements. The DCS, developed at the NASA Goddard Space Flight Center, consists of five spacecraft control modes and six test mass control modes, combined into six "DRS Mission Modes". Attitude Control and Zero-G were primarily used to control the spacecraft during initial handover and during many of the CMNT characterization experiments. The other Mission Modes, Drag Free Low Force, 18-DOF Transitional, and 18-DOF, were used to provide drag-free control of the spacecraft about the test masses. This paper will discuss the performance of these DCS spacecraft and test mass control modes. Flight data will be shown from each mode throughout the mission, both from nominal operations and during various flight experiments. The DCS team also made some changes to controller, filter, and limit parameters during operations; the motivation and results of these changes will be shown and discussed.

1. Introduction

The Space Technology-7 Disturbance Reduction System (DRS) is a project managed by the NASA Jet Propulsion Laboratory that is an experiment package aboard the European Space Agency (ESA) LISA Pathfinder (LPF) spacecraft (pictured in Fig 1), which launched from Kourou, French Guiana, on December 3, 2015. The purpose of DRS is to validate two specific technologies: colloidal micro-Newton thrusters (CMNTs) to provide low-noise six degree-of-freedom control of the spacecraft, and drag-free control algorithms [1]. The CMNT system was developed by Busek Inc., and the Dynamic Control System (DCS) algorithms and flight software for drag-free control were developed at the NASA Goddard Space Flight Center. The DRS uses highly sensitive drag-free sensors (DFS), which are provided by the LISA Technology Package (LTP) [2], to validate its technologies.

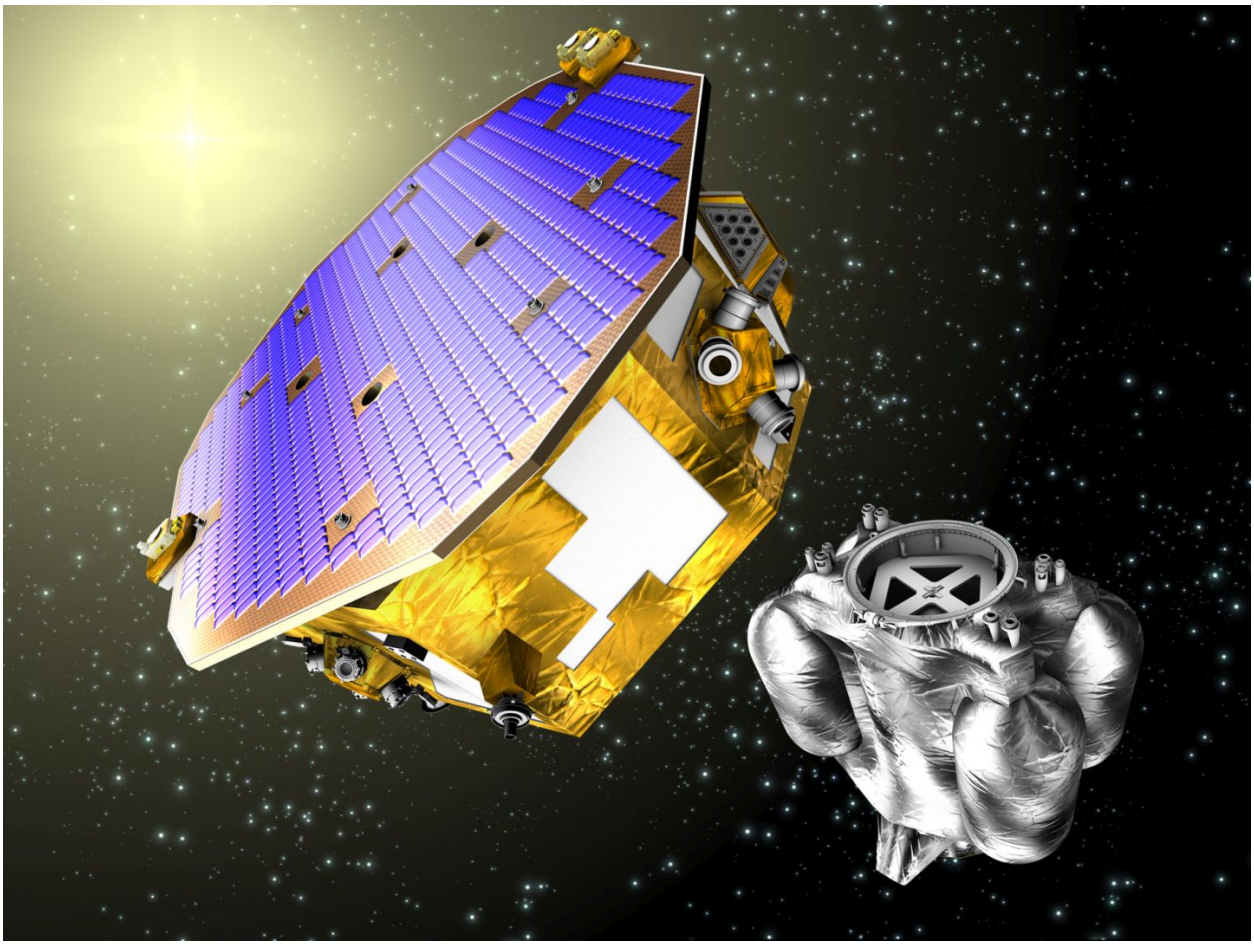

Fig 1. LISA Pathfinder Post-Propulsion Module Separation (ESA).

DRS started its operations on August 14, 2016, after three commissioning periods during which all control modes were successfully tested [3]. The DCS algorithms were designed to enable DRS to meet its attitude control and drag-free operation requirements. The primary requirements of the attitude control system (ACS) are to maintain the pointing of the Z-axis (the axis normal to the solar array) within a 2° half-cone of the Sun and maintain the rotation about the Z-axis to within 2° of a target attitude. The primary requirement for drag-free operation of DRS is to maintain the spacecraft's position with respect to a single free-floating test mass to better than 10nm/$\sqrt{Hz}$, along the sensitive axis (the axis connecting the two test masses), over the frequency range of 1–30 mHz. There is also a requirement to maintain the spacecraft's position with respect to two free-floating test masses to better than 10nm/$\sqrt{Hz}$, along the sensitive axis, with a goal of limiting the residual accelerations of those test masses to below $3\text{x}10^{-14}$ (1 + [f/3 mHz]²) m/s²/$\sqrt{Hz}$, over the frequency range of 1–30 mHz. There were also a number of derived requirements on the test mass control systems necessary to be able to successfully control the test mass position and attitude within their housings.

This paper will discuss the time-domain performance of all of the DCS spacecraft and test mass control modes. The performance of the spacecraft and test masses in drag-free operation will be shown, but because the requirements for drag-free operation are only applicable in the frequency range of 1–30 mHz, these requirements cannot be verified just by direct examination in the time domain. The performance of the DCS algorithms with respect to the drag-free requirements is shown in [4].

2. LISA Pathfinder/Disturbance Reduction System Configuration

When initially formulated, DRS was meant to be a parallel experiment to be flown on the ESA Small Missions for Advanced Research in Technology-2 (SMART-2) mission. The initial configuration of the SMART-2 mission, renamed LISA Pathfinder (LPF) in 2004, is shown in Fig 2. In this configuration the ESA contributions are shaded in blue and the NASA contributions are shaded in red. Each half of the mission includes attitude and drag-free control algorithms, a gravitational reference sensor, and microNewton thrusters. From the standpoint of spacecraft

control, the only shared component was for the DRS to be provided spacecraft attitude information from the LPF star tracker, along with the target attitude. In this configuration, the overall DRS project was managed by JPL, with Goddard Space Flight Center (GSFC) developing the spacecraft attitude and drag-free control algorithms and software, Busek providing the Colloidal MicroNewton Thrusters, and Stanford University providing the Gravitational Reference Sensor (GRS). In this configuration, the test mass control algorithms were being designed and implemented by Stanford.

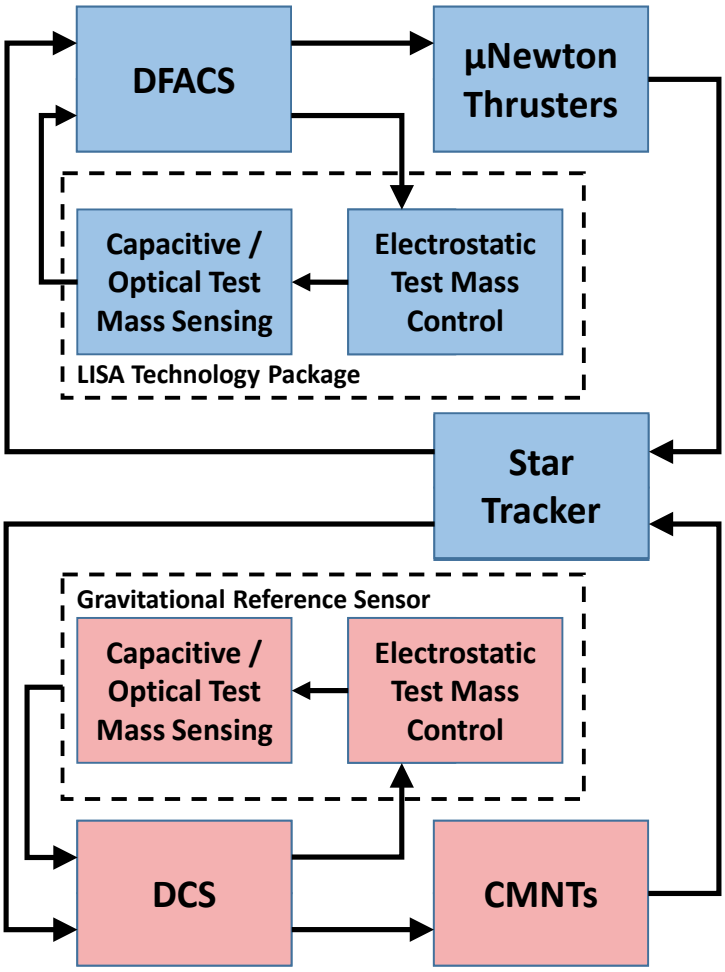

Fig 2. Original LPF/DRS Configuration

When the GRS was descoped, the new configuration of the overall LPF mission became what is shown in Fig 3. In this configuration, the NASA contribution is two clusters of four CMNTs, the DCS algorithms and software, and the Integrated Avionics Unit (IAU) and command and data handling software needed to interface with the CMNTs and the LPF. Both spacecraft and target attitude information and test mass position and attitude information is passed to the DRS from LPF, and, in turn, force and torque commands to the test masses are passed back. With this descoped option, the scope of worked required from GSFC for the DCS actually increased, with the added responsibility of designing the test mass control algorithms for the use of the LTP instrument. (In addition to the GRS descope, a later descope of a backup thruster system on the LPF side of the spacecraft necessitated the addition of the ability of LPF to command the DRS CMNTs as a backup for propulsion module separation and for nominal operations. This is denoted by the dashed line in Fig 3.)

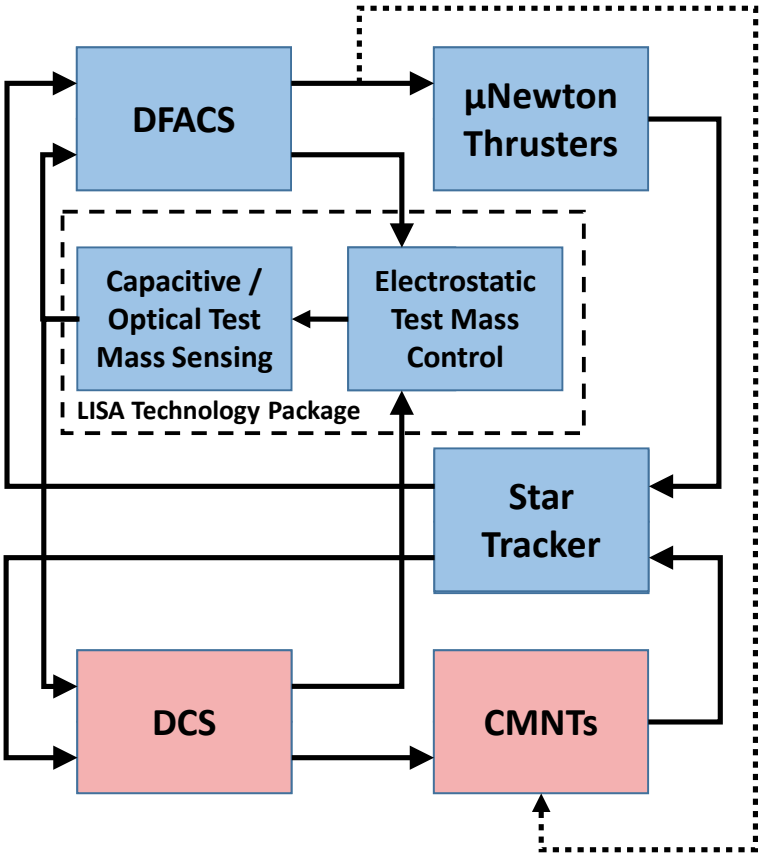

Fig 3. LPF/DRS Configuration after GRS Descope

Two aspects of the DRS system had implications for the DCS design. First, because of the way the CMNTs function [5], in operation each thruster has both a minimum and a maximum thrust. Each thruster must be set at a bias level with sufficient room for positive and negative variations in order to be able to provide the commanded forces and torques to the spacecraft. Second, because each four-thruster CMNT cluster has two Sun-facing thrusters and two Sun-opposed thrusters, the bias level on the Sun-opposed thrusters needs to be significantly higher than that of the Sun-facing thrusters in order to counteract the solar radiation pressure (SRP) on the spacecraft. From the viewpoint of conserving propellant, it was desirable to set these bias levels as low as possible, though they needed to be high enough to allow for control variations.

Another thing to keep in mind is the coordinate definitions used. As mentioned above, the Z-axis is normal to the solar array, with the positive Z-axis nominally pointing at the Sun. The X-axis is the axis connecting the two test masses, and is referred to as the sensitive axis. Positive X points through Test Mass 1 to 2. Because DRS only had two clusters of four thrusters, placed on opposite sides of the spacecraft on the X-axis, this axis was also the axis about which DRS had the least attitude control authority.

3. Dynamic Control System Mode Design

Fig 4 shows the mode design of the DCS at the time of LPF launch. The DCS team had always been responsible for design of the spacecraft control modes, shown in the second column of Fig 4. When the GRS was descoped and the responsibility of controlling the LTP test masses was added to the DCS, an analogous mode design was used, with many similar mode names prefixed with DFS for “Drag Free Sensor”. In addition to the control mode used for each test mass, it was necessary to set the “force mode” used. When the DCS was designed, it was assumed that the LTP would have a high force mode and a low force mode. The high force mode had greater control authority, while the low force mode had significantly better noise performance. As the design of the LTP sensor matured, the name for the high force mode became Wide Range and for the low force mode became High Resolution. Also, as discussed below, one of the test masses is designated the Reference Test Mass (RTM) and one as the Non-Reference Test Mass (NTM).

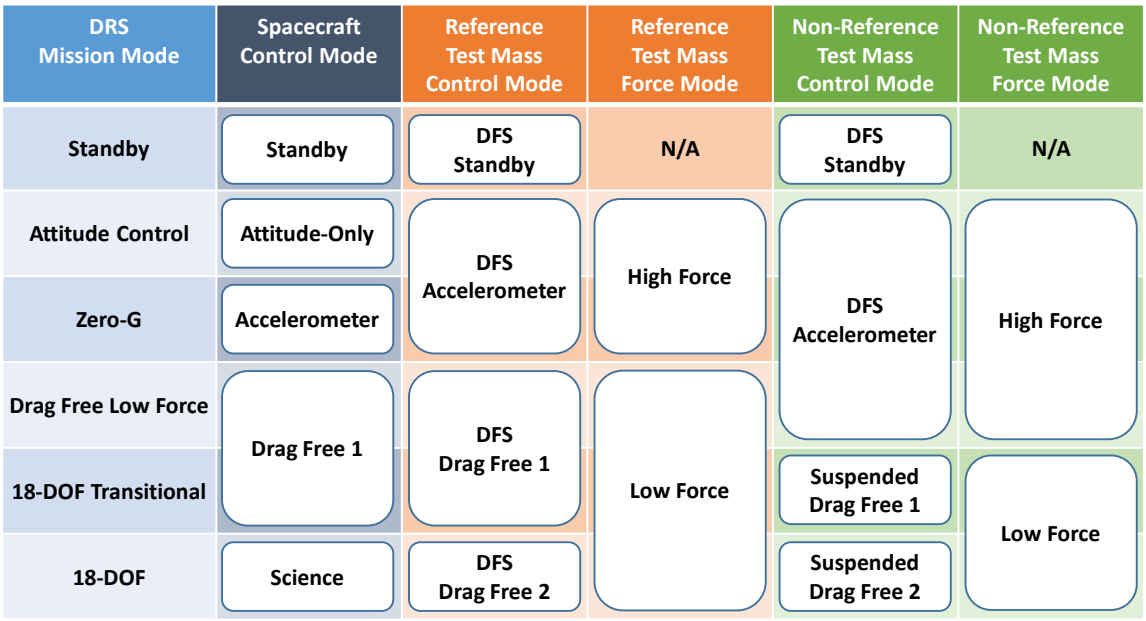

Fig 4. DCS Spacecraft and Test Mass Control Mode Design

The combination of spacecraft control mode, RTM control mode and force mode, and NTM control mode and force mode made up what was called the DRS Mission Mode. The purpose of each of the five DRS Mission Modes (other than Standby) was as follows.

The purpose of the Attitude Control Mission Mode is attitude control of the spacecraft using the Attitude-Only spacecraft control mode, and was used for initial handover from LPF control. In this mode, the two test masses are kept centered in their housings using DFS Accelerometer mode in High Force. While Attitude Control does not counteract any of the SRP directly, it is possible to counteract much of the SRP force on the spacecraft through selection of the thruster biases. The DRS team was asked by the spacecraft controllers to try to counteract as much of the SRP force as possible in order to minimize disturbances to the spacecraft orbit.

In the Zero-G Mission Mode, control of the test masses remains the same. The spacecraft control mode changes to Accelerometer, which is the same attitude controller as Attitude-Only, with the addition of spacecraft force control commands via the thrusters to minimize the electrostatic force commands applied to the RTM. By trying to minimize the forces needed to keep the RTM centered in its housing, this mode is essentially trying to cancel out the low frequency disturbance forces and torques on the spacecraft, as well as differential gravity and other secular effects on the RTM. In initial operations, the biases were set to cancel out only about 80% of the expected SRP force, but as the team gained more experience with operating the spacecraft, the biases were chosen to compensate for more of it.

The Drag Free Low Force Mission Mode is the first mode implementing full drag-free operation. In this mode, the force mode of the RTM is switched to Low Force in order to improve noise performance. The DFS Drag Free 1 control mode zeroes out force commands to the RTM in all axes, only controlling RTM attitude. Meanwhile, the Drag Free 1 spacecraft control mode uses the CMNTs to fly the spacecraft around the RTM.

Finally, the 18-DOF Transitional and 18-DOF Mission Modes are used to bring the NTM “online” for drag-free operation. In 18-DOF, the force commands to the NTM in the sensitive axis are only applied below the measurement band of interest, 1–30 mHz, allowing the spacecraft to fly drag-free about both test masses within that band. 18-DOF Transitional is a transitional mode to get into 18-DOF, in which the NTM Force Mode is changed to Low Force.

It is interesting to note that the DRS Drag Free Low Force, 18-DOF Transitional, and 18-DOF modes are the only control modes that fly the spacecraft drag-free in all axes. The corresponding Drag Free and Attitude Control System (DFACS) modes on the LPF side of the spacecraft are only drag-free in the sensitive axis.

For full details of the spacecraft and test mass control design for each mode, see [5]-[8].

4. Dynamic Control System Performance

The rest of this paper will discuss the time-domain performance of the DCS. In all cases but one, the DCS controllers satisfied all attitude control and drag-free requirements for spacecraft and test mass control, so these requirements will not be addressed specifically. Features of interest for the experiments will be discussed, as well as describing the several control system adjustments that were made during the course of operations.

4.1 Attitude Control and Zero-G

As discussed above, the first two DCS Mission Modes were Attitude Control and Zero-G. Attitude Control was used as a transitional mode for initial handover to DRS control of the LPF. In order to minimize disturbances to the spacecraft orbit, it was desirable to transition into Zero-G as soon as possible, since this mode counteracts the SRP force on the spacecraft. After the descope of the NASA gravitational reference sensor, the main focus of the DRS mission became characterization of the CMNTs. Many of the experiments for characterizing these thrusters were performed in Zero-G.

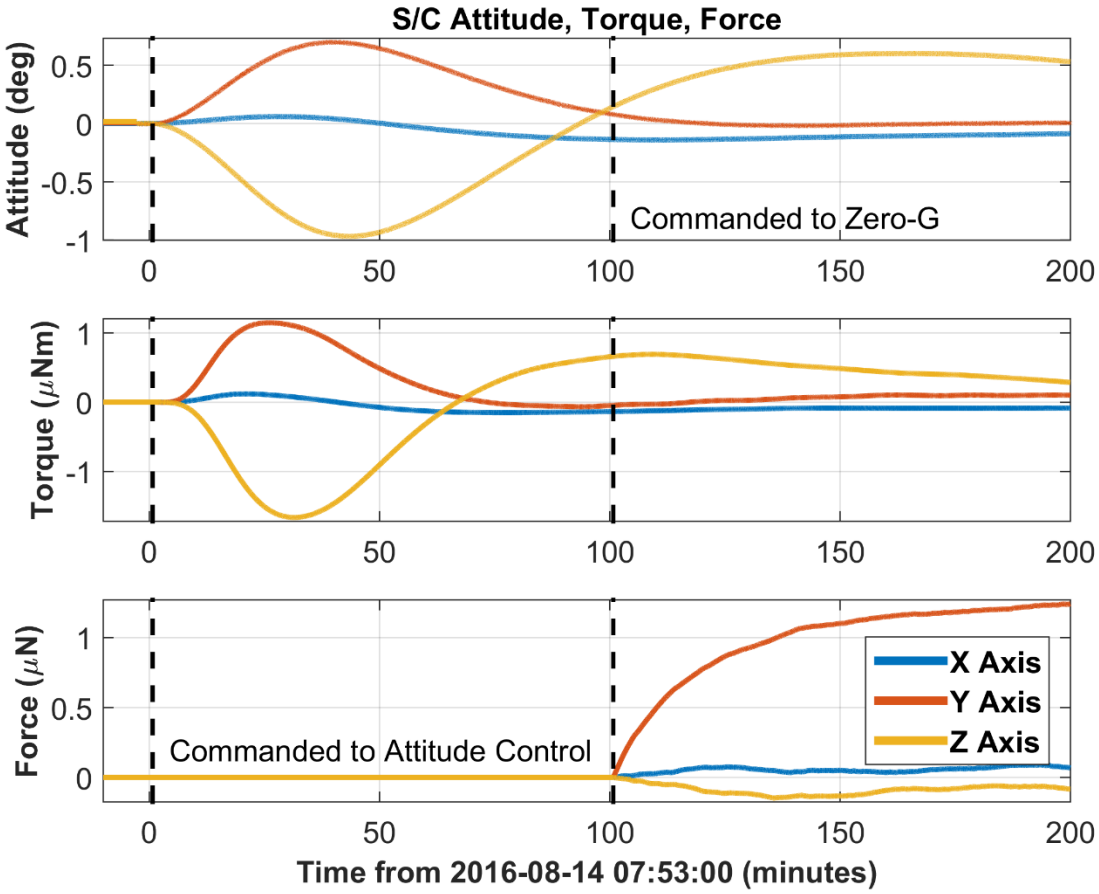

Fig 5. Spacecraft Attitude and Commanded Torque and Force for Attitude Control and Zero-G

Fig 5 shows the spacecraft attitude and the commanded torques and forces for the Attitude Control and the beginning of the Zero-G portion of a full run into 18-DOF. Spacecraft attitude performance remains within required limits. Upon the transition to Zero-G, torque commands stay on essentially the same trajectory, confirming that the spacecraft attitude control in the first two modes is the same. However, force commands begin to ramp up in order to try to minimize electrostatic commands to the RTM (for all experiments discussed in this paper, test mass 1 (TM1) was used as the Reference Test Mass). Note that these force commands are applied on top of the open-loop spacecraft force produced from the default thruster bias levels. As can be seen from the fact that the Z-axis force command is fairly low, at this point in the mission the thruster biases are already accounting for much of the

approximately 26 μN solar radiation pressure force. Fig 6 shows the thruster commands during this run. The four thrusters at a higher bias are the Sun-opposed thrusters and the others are the Sun-facing ones.

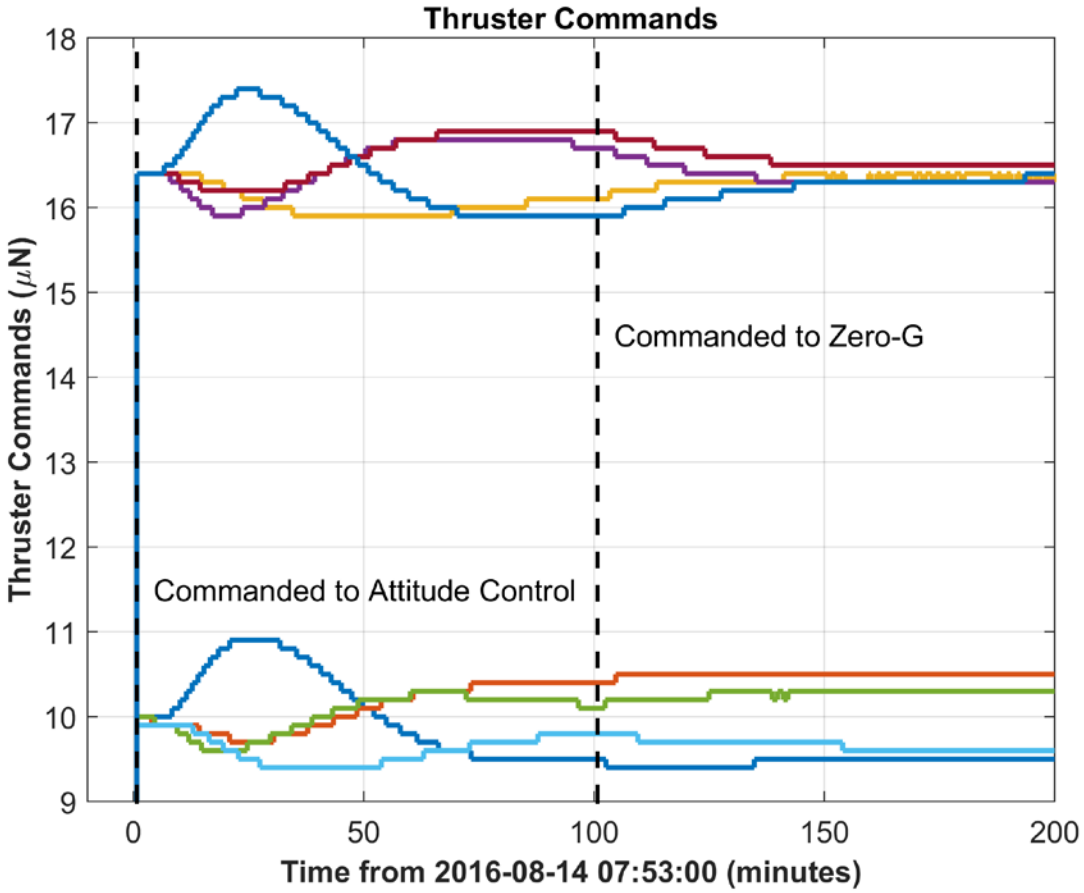

Fig 6. Thruster Commands for Attitude Control and Zero-G

In both the Attitude Control and Zero-G Mission Modes, both test masses are being controlled with DFS Accelerometer mode in High Force. Fig 7 shows the control of the RTM. The largest attitude and position excursions of both test masses occur when control of the test masses is handed to DRS at the beginning of the run, but the control system quickly brings them under control. Upon transition into Zero-G, note that the force being applied to TM1 in all axes goes towards zero. Because TM1 is the reference in this case, one of the goals of Zero-G is to apply thruster force commands to the spacecraft in order to minimize these test mass force commands. Plots of the attitude, position, and commanded torque and force for TM2 for this run would look similar to TM1, except that since TM2 is not the reference, the force commands would not necessarily go to zero, as the non-common mode forces/accelerations are not compensated.

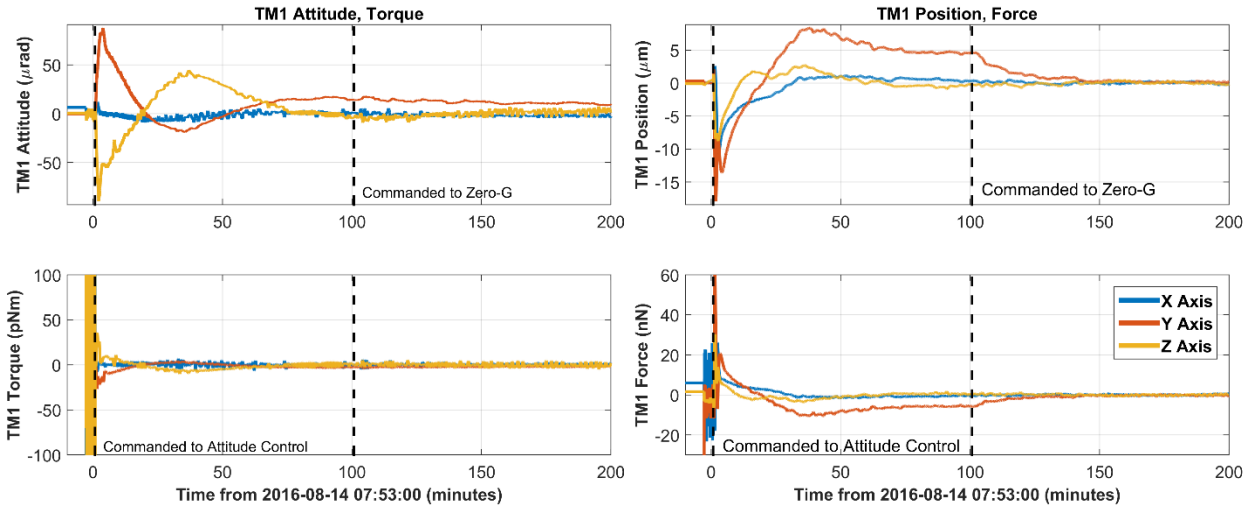

Fig 7. Test Mass 1 Performance for Attitude Control and Zero-G

Zero-G was used to run many of the thruster characterization experiments, used to characterize the performance, timing, thrust noise, and other parameters of the CMNTs. The thruster characterization experiments that were run, after the spacecraft was settled in Zero-G, include injecting sine or square wave signals on top of the command to one or more thrusters, freezing one thruster at its current value, allowing the other thrusters to adjust, freezing all thrusters at their current value (using existing fault detection to re-enable close-loop control if attitude limits were exceeded), and running tests at several thruster bias levels to see how that affected noise performance. Fig 8 and Fig 9 show an example of Zero-G performance for one of these experiments, showing the thruster commands and the position and force commands sent to both test masses during a sine wave signal injection of Thruster 7, one of the Sun-opposed thrusters. The spacecraft and test mass attitude plots are not shown for this run since the attitude performance is not substantially affected by the signal injection. As can be seen in Fig 9, though, the injection is visible in the positions and commanded forces to both test masses.

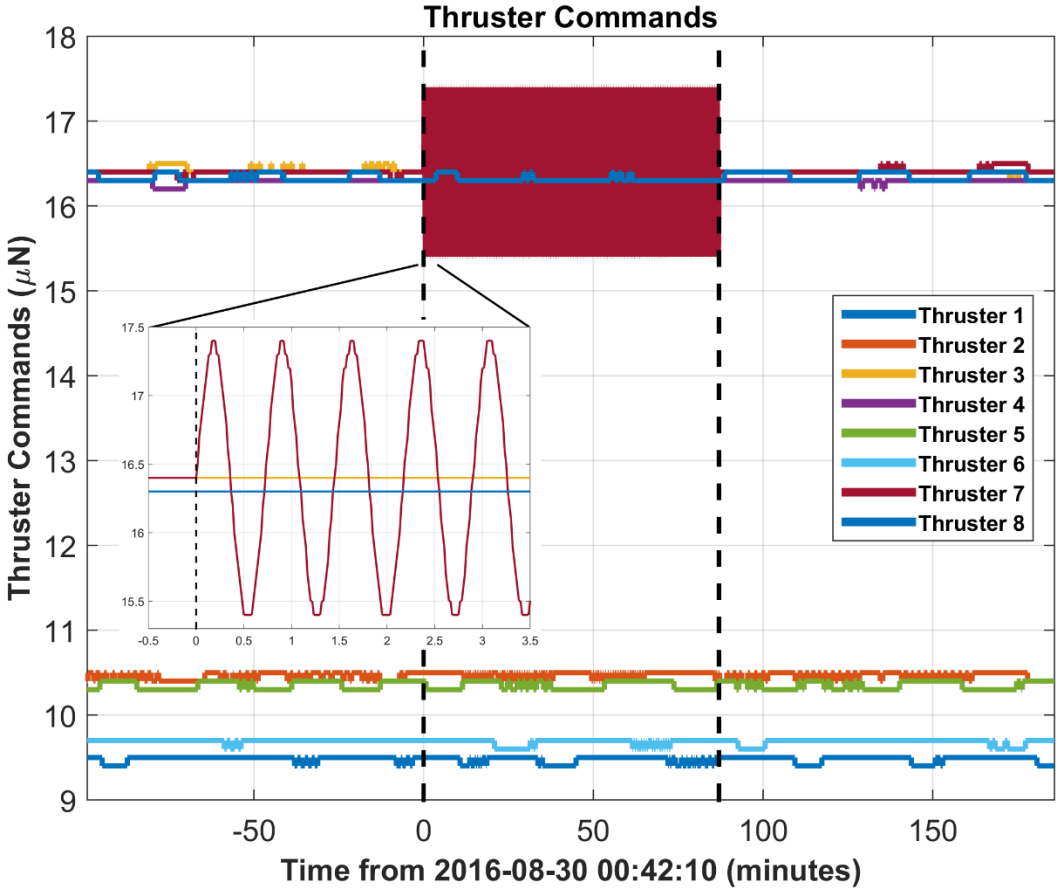

Fig 8. Thruster Signal Injections in Zero-G

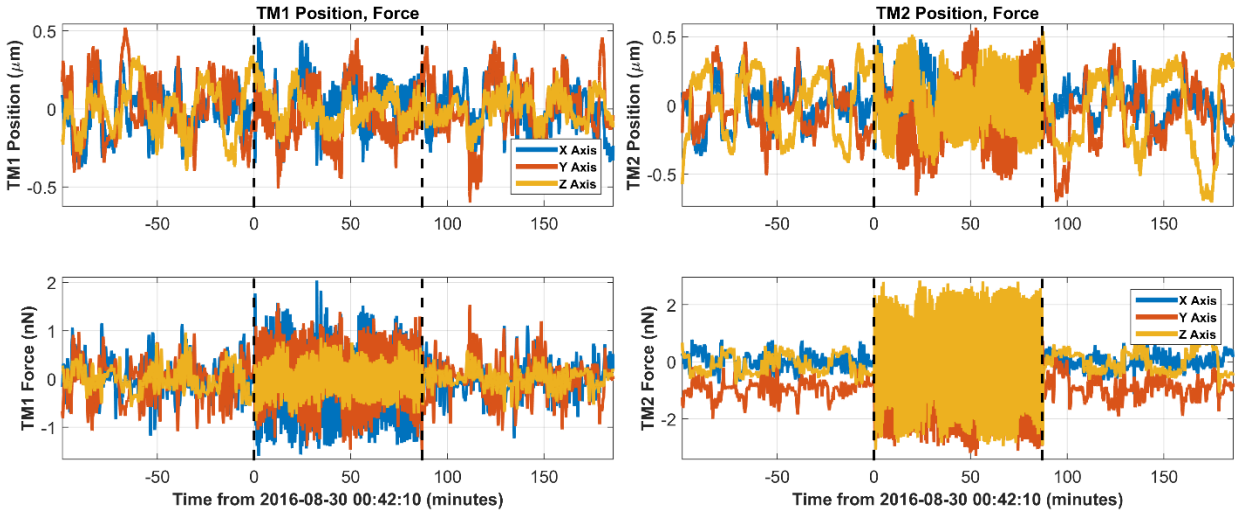

Fig 9. Test Mass Position Performance During Thruster Signal Injections in Zero-G

4.2 Drag Free Low Force

After Attitude Control and Zero-G, the next Mission Mode is Drag Free Low Force. Unfortunately, as shown in the thruster commands in Fig 10, the initial transition into this mode was not successful. After only four minutes,

spacecraft fault detection triggered an autonomous transition back into Zero-G where control was re-established. The behavior at transition into Drag Free Low Force was attributed to the initialization transients of a rate filter in the drag-free controller, which uses the sensed test mass position errors. As shown earlier in the control mode design diagram (Fig 4), upon transition to Drag Free Low Force, the RTM control was switched to DFS Drag Free 1 while simultaneously being switched into Low Force. However, the command interface between the DRS and the LTP did not allow for those two transitions to be simultaneous. The DFS Drag Free 1 controller has a relatively large bandwidth compared to the attitude controller in order to meet the drag-free requirements below 30 mHz, so any transients into the controller can affect the response adversely. Analytical simulations and simulations on the real-time testbeds at NASA and ESA had confirmed the existence of transients at this mode transition, but they had never caused instability. The likely cause of deviation from past behavior may have been due to slow thruster response from Thruster 1 as well as other differences in the behavior of the flight system compared to the testbeds used for timing of LTP commands.

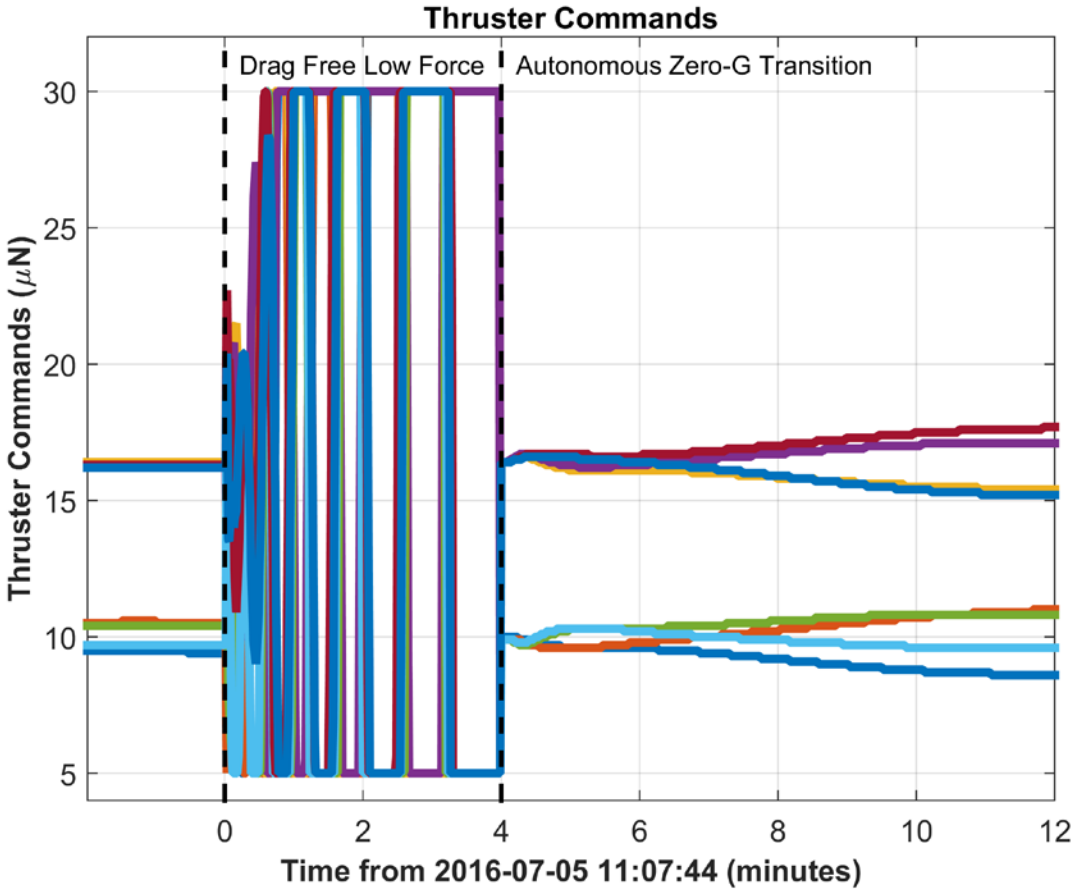

Fig 10. Thruster Commands for Unsuccessful Transition to Drag Free Low Force

A two-pronged approach to reduce the DCS command variations at the transition was implemented for the next transition into Drag Free Low Force. First, the timing of the test mass transitions into Low Force mode was changed. The RTM was switched into Low Force mode fifteen minutes before the command into Drag Free Low Force. The early transition allowed any RTM attitude and position transient to settle out before going to Drag Free Low Force. Additionally, in anticipation of easing the transition into the 18-DOF Transition Mission Mode, the NTM was switched into Low Force fifteen minutes after going to Drag Free Low Force. Additionally, the Drag Free 1 spacecraft control system was changed via table update to limit spacecraft force commands to 5 µN per axis. The limits served to further cap the variations in the thrust commands, reducing dynamic demand on Thruster 1. After these changes were made, Drag Free Low Force operated successfully throughout the mission. (See [3] for further discussion.)

Fig 11 and Fig 12 show the spacecraft attitude performance and RTM attitude and position at the transition into Drag Free Low Force. The differences in the use of the force command on the spacecraft can easily be seen at the transition. Before the transition into Drag Free Low Force, in Zero-G, the force command to the spacecraft is used to minimize the low frequency force command applied to the RTM. Hence, the force commands vary fairly slowly. After the transition into Drag Free Low Force, there is no longer any force command sent to the RTM (as shown in Fig 12) and the spacecraft force commands show significantly more variations as they are used to fly the spacecraft around the RTM using a considerably higher bandwidth control.

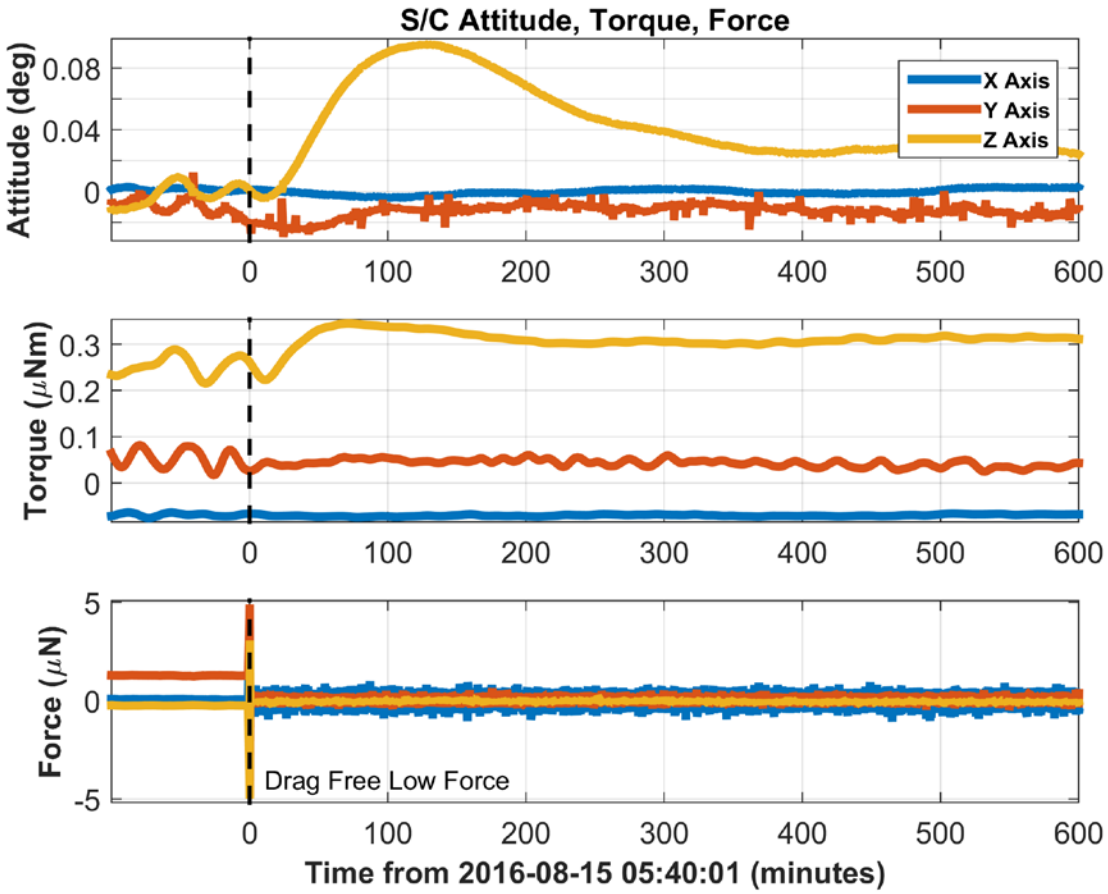

Fig 11. Spacecraft Attitude and Commanded Torque and Force for Drag Free Low Force

The other thing that can be seen in Fig 12 is the transition into Low Force mode for the RTM fifteen minutes before the Mission Mode is changed to Drag Free Low Force. This transition causes a transient in both the measured test mass attitude and position, but the better noise performance of Low Force can be seen in the attitude performance and torque commands.

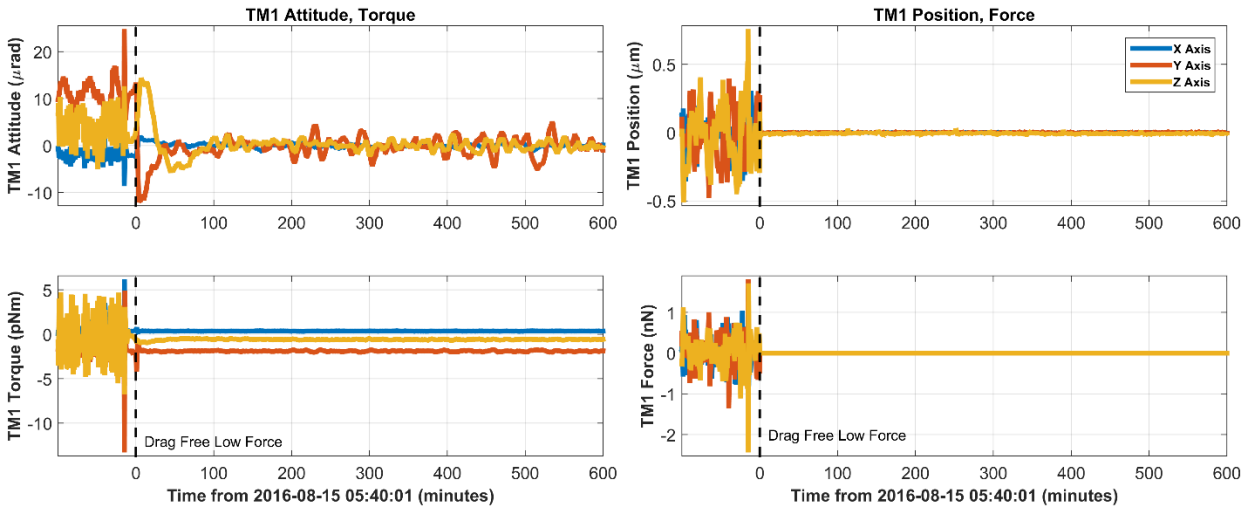

Fig 12. Test Mass 1 Performance for Drag Free Low Force

Fig 13 and Fig 14 show the transition into Drag Free Low Force, showing the attitude, position, and torque and force commands for both test masses thirty minutes before and after the transition. The TM1 plots clearly show the transition into Low Force mode on the RTM ten minutes before Drag Free Low Force is commanded and the TM2 plots show the transition into Low Force mode on the NTM ten minutes after.

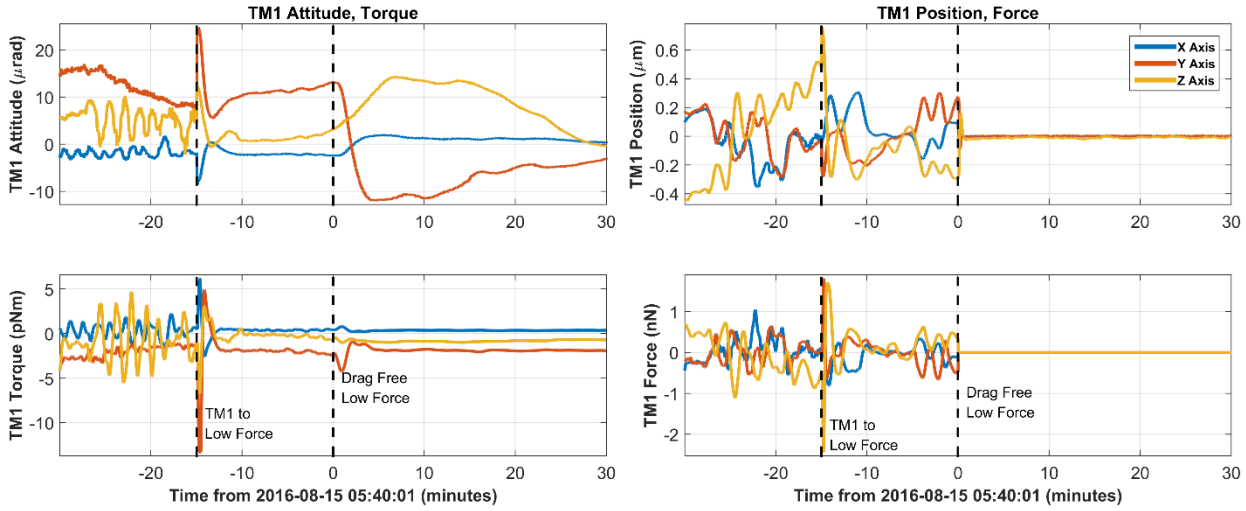

Fig 13. Test Mass 1 Force Mode Transition for Drag Free Low Force

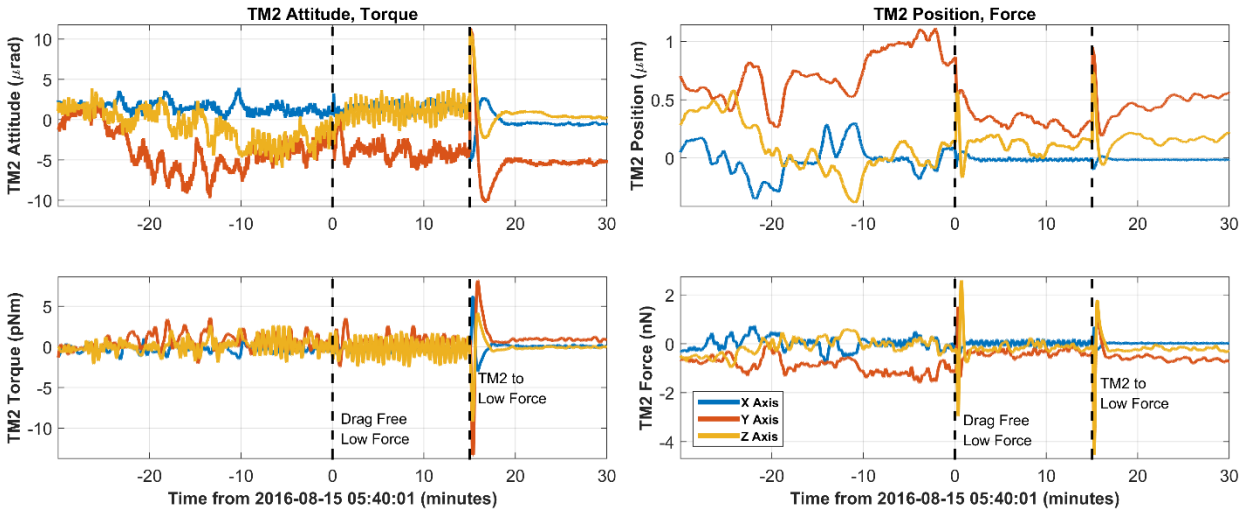

Fig 14. Test Mass 2 Force Mode Transition for Drag Free Low Force

4.3 18-DOF Transitional and 18-DOF

The final two Mission Modes, 18-DOF Transitional and 18-DOF, will be discussed together. 18-DOF represents that full "Science" mode of DRS, allowing the spacecraft to fly drag-free about both test masses along the sensitive axis within the measurement band of 1–30 mHz. When the NASA GRS was descoped, no requirements for the performance of this mode remained, since the performance primarily depended on the LTP sensor. However, DRS maintained a goal of meeting the acceleration specifications on both test masses. None of the DRS requirements required any mode beyond Drag Free Low Force to be verified. However, the DRS 18-DOF mode was the closest to the DFACS mode used to perform the majority of their operations, and data taken during the run offered one of the best opportunities for comparing the operation of the DRS CMNTs and control laws to the DFACS and LPF cold-gas microNewton thrusters.

As shown in Fig 3, the LTP sensor has both capacitive and optical measurements of the test mass position and attitude. The capacitive measurements give attitude and position measurements of each test mass in all degrees of freedom. In addition, the Optical Metrology System (OMS) uses laser interferometry to provide measurements for three degrees of freedom for each of the two test masses; the position along the sensitive axis as well as the rotation about the two transverse axes. The initial design of the DRS flight software did not support use of the measurements from the OMS, but this capability was added before DRS operations.

4.3.1 Using Capacitive Sensing in All Axes

Fig 15 shows the spacecraft attitude performance upon the transition into 18-DOF Transitional and 18-DOF Mission Modes. Recalling from Fig 4 that the spacecraft control mode does not change going from Drag Free Low Force to 18-DOF Transitional, it is not surprising that there is no apparent change in the attitude performance until the system transitions into 18-DOF. The spacecraft torque commands required to fly the spacecraft drag-free about one RTM degree of freedom (the attitude about the X-axis) and drag-free in the lateral axes of the NTM (Y- and Z-axis translations), in the measurement band of interest, are much more dynamic, as can be seen both in Fig 15 and in the resulting thruster commands in Fig 16. It should be noted that spacecraft drag-free control cannot follow the NTM along the sensitive axis, as it can only follow one test mass (RTM, in this case). Hence, a very soft electrostatic suspension loop is used to control the NTM along the sensitive axis, below the measurement band.

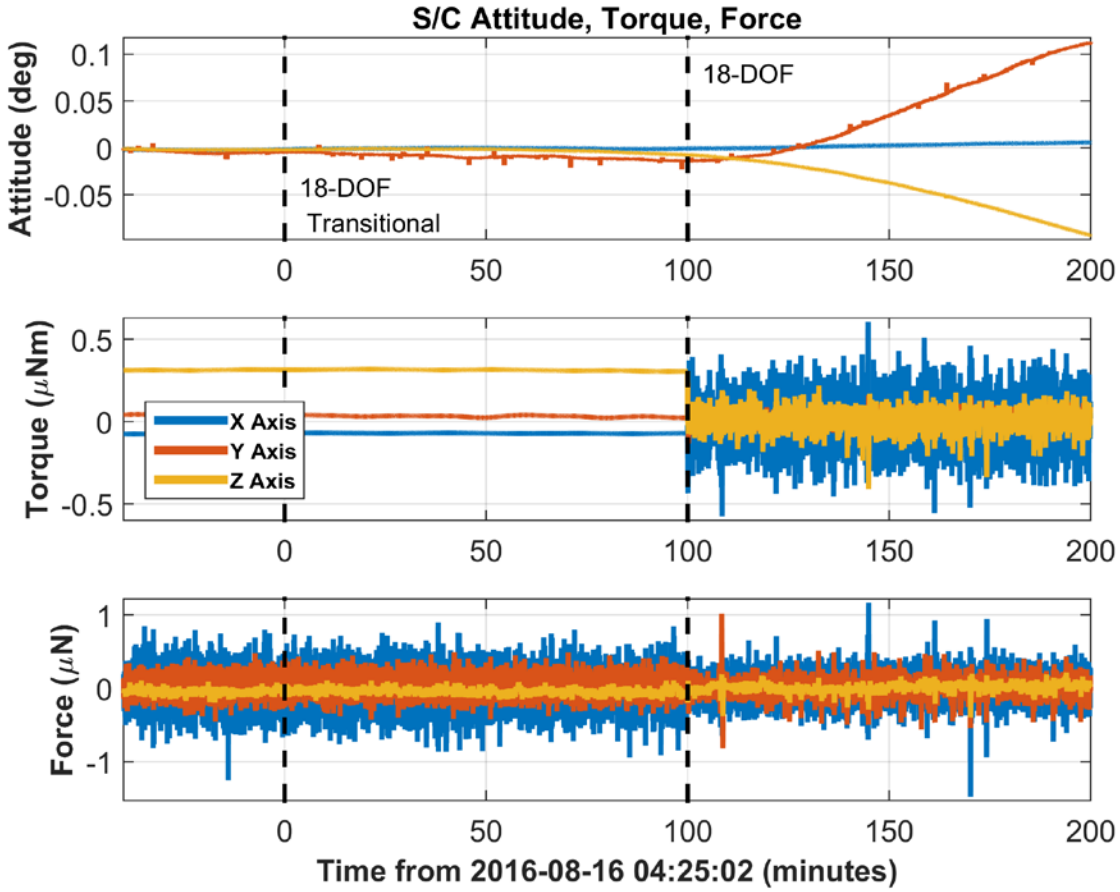

Fig 15. Spacecraft Attitude and Commanded Torque and Force Transitioning into 18-DOF

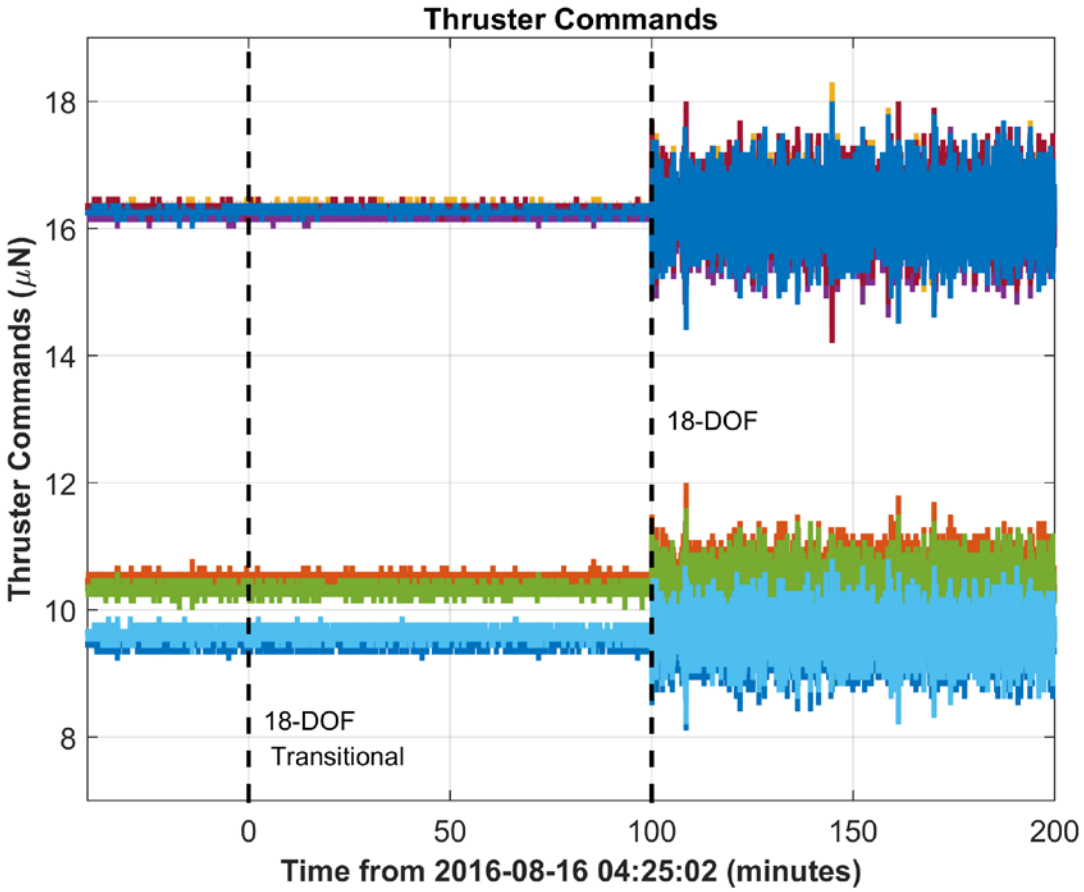

Fig 16. Thruster Commands Transitioning into 18-DOF

Fig 17 and Fig 18 show the attitude and position performance of both test masses upon transition into 18-DOF. As expected, RTM performance is the same until the transition to 18-DOF, since the same RTM controller is used in 18-DOF Transitional and Drag Free Low Force. NTM performance changes significantly in 18-DOF Transitional, as the test mass is brought into a state where it can successfully transition into the full 18-DOF Mission Mode.

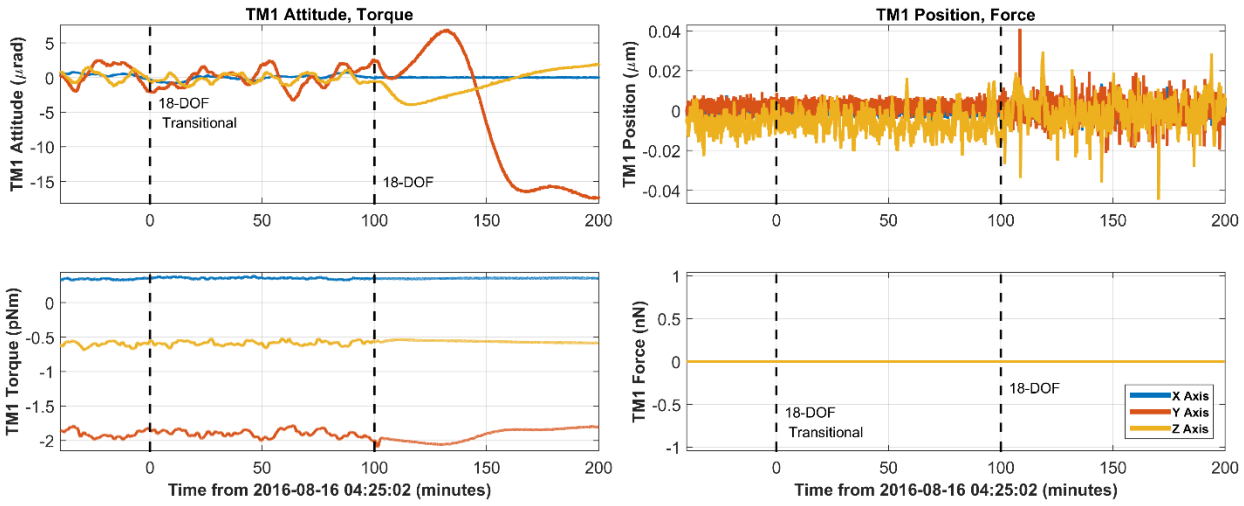

Fig 17. Test Mass 1 Performance Transitioning into 18-DOF

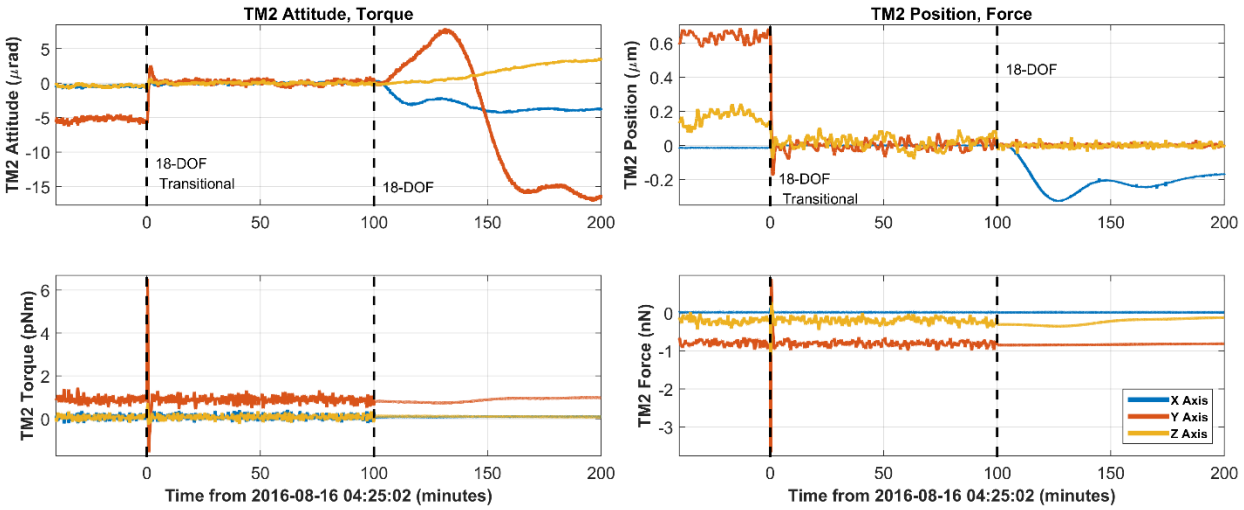

Fig 18. Test Mass 2 Performance Transitioning into 18-DOF

Fig 19 shows the spacecraft attitude performance in 18-DOF over approximately 34 hours. The softness of the control in this mode can be easily seen by the fact that it takes almost the entire 34 hours to bring the attitude transient back down. The main reason behind soft controllers, except for drag-free control, is to limit the cross talk that may bleed into the sensitive axis from other degrees of freedom.

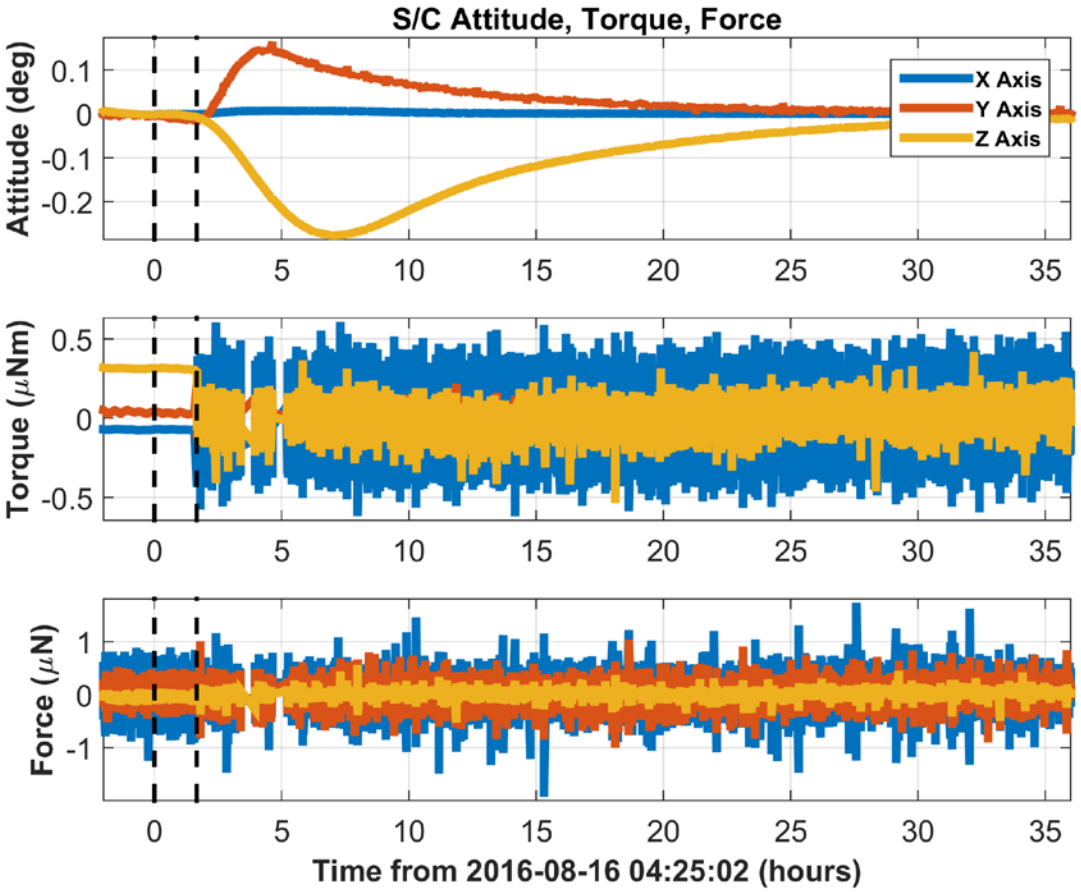

Fig 19. Spacecraft Attitude and Commanded Torque and Force for 18-DOF

4.3.2 Using Optical Metrology System Sensing

One of the first improvements implemented for the operation of the 18-DOF Mission Mode was to make use of the OMS measurements in the applicable axes of the test mass position and attitude. Fig 20 shows the test mass position and attitude measurements upon this transition. After the transition to OMS measurements, the X-axis position measurement and Y- and Z-axes attitude measurements for both test masses are from the OMS laser interferometry measurements. It is possible to see in the figure the transients upon the change, due to slightly different null points for the capacitive and optical measurement systems, as well as some of the measurements being visibly smoother.

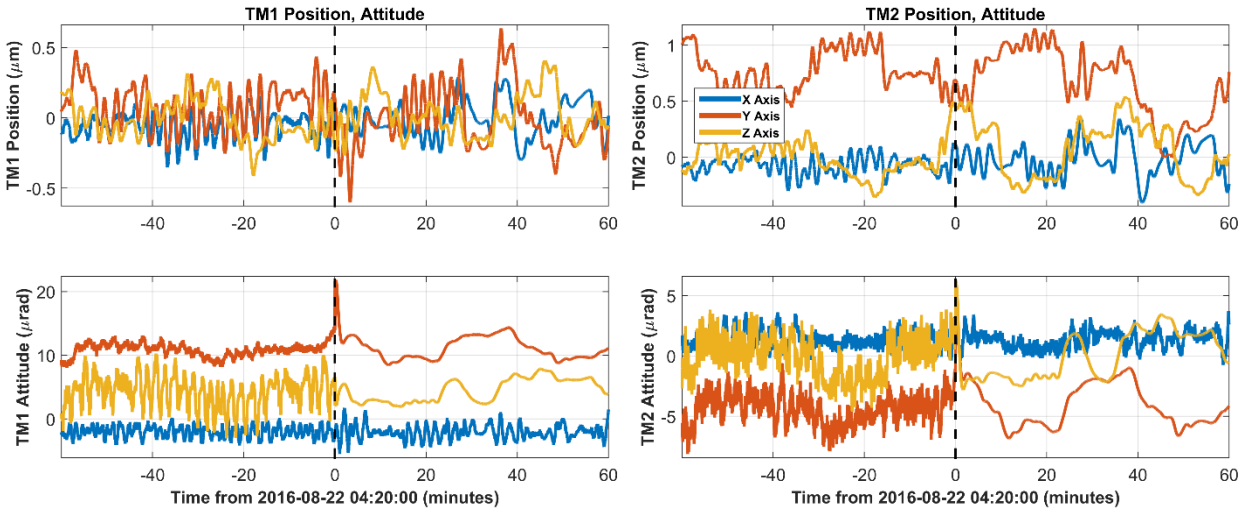

Fig 20. Test Mass Position and Attitude Measurements on Transition to OMS Sensing

Fig 21 shows the spacecraft attitude performance for a similar time period to the 18-DOF experiment shown in the previous section that used purely capacitive measurements. The behavior of the spacecraft attitude and control torques and forces is not visibly different in the time domain from the previous run. One interesting feature of this experiment that occurs approximately seven hours after the transition into 18-DOF Transitional is a spike in commanded torque and force. This spike also appears in the position and force command data for both test masses and is believed to be a potential impact from a micro-meteoroid.

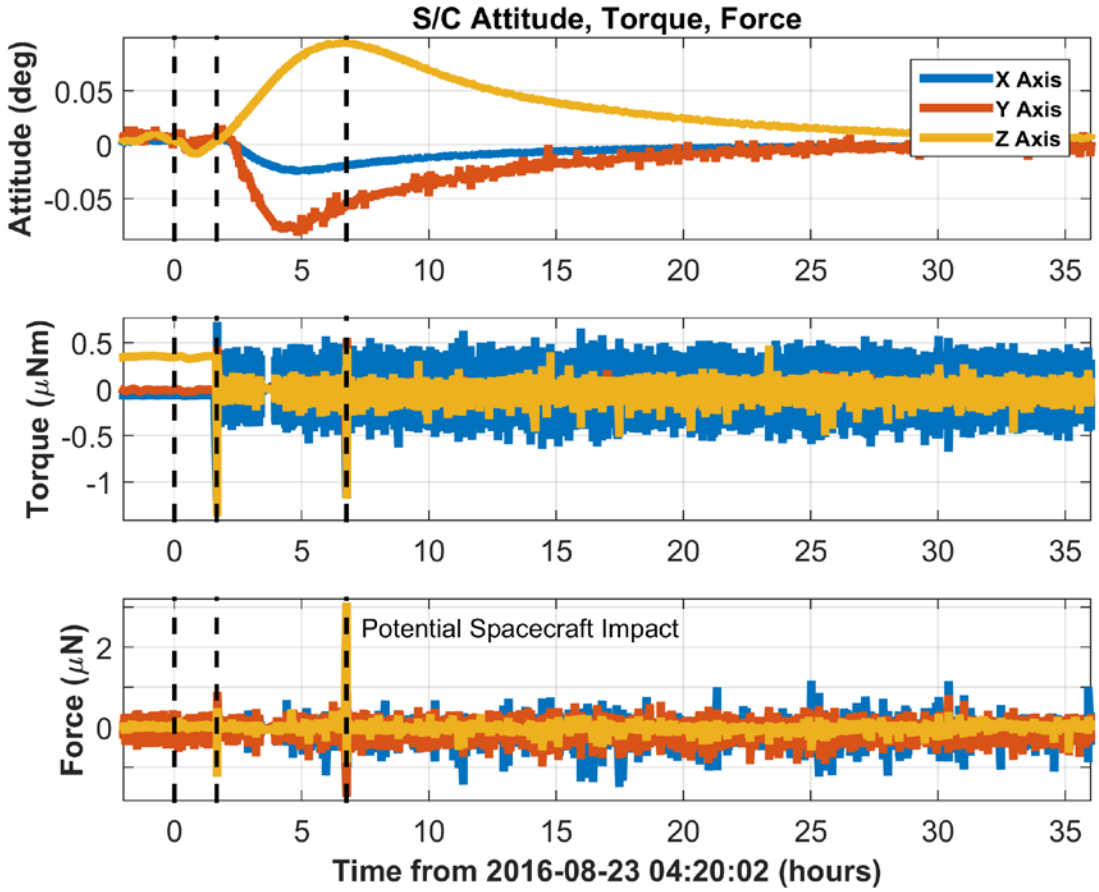

Fig 21. Spacecraft Attitude and Commanded Torque and Force for 18-DOF with Optical Sensing

Fig 22 shows a side-by-side comparison of the RTM position and attitude for just the axes that can be sensed by the OMS. The plot on the left is from the 18-DOF experiment using only capacitive sensing while the one on the right is from the experiment using the OMS. While the performance difference is clearer when viewed by taking power spectral densities and looking in the measurement band of interest [4], it can be seen by looking at the time-domain plots shown below that the performance when using the OMS measurements has better position and attitude performance.

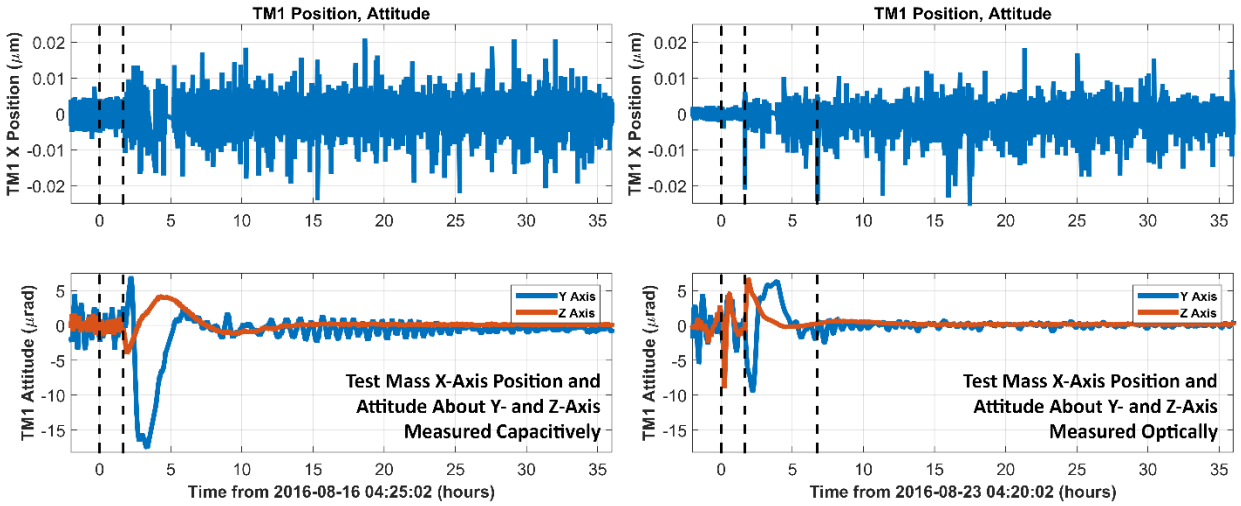

Fig 22. Test Mass 1 Control Performance for Capacitive vs Optical Sensing

4.3.3 Change of Test Mass 2 Sensitive Axis Position Reference

One of the things that the DCS learned about the design of the DFACS control system on the LPF is that their full drag-free mode differed in one respect from that of the DCS 18-DOF mode. In the DCS, the position measurement of the NTM, as with the RTM, was referenced to the center of its housing in all axes. In the DFACS, the position measurement of the NTM in the sensitive axis was referenced to the RTM. Referencing the position measurement of the NTM to the housing results in the spacecraft motion being present in the feedback loop for the NTM position control, potentially resulting in a higher response in position control. With the use of the OMS for position measurements in the sensitive axis, it was straightforward to test the DCS using the same NTM position reference as the DFACS. Running in this configuration did not result in substantial differences in the time-domain performance of the DCS, but there were measurable performance differences in the frequency domain [4].

4.3.4 Use of Reduced Electrostatic Test Mass Actuation Levels

During the nominal LPF mission, which was completed before DRS commissioning and operations, one of the changes the LPF Science Team examined as they ran their experiments was to use progressively lower actuation limits of the two test masses. Lower actuation limits improved the noise performance of the LTP and reducing these levels was directly reflected in the system-level noise performance. The final actuation levels used by LPF was dubbed “URLA”, or Ultra-Ridiculously Low Actuation. During DRS operations, the DRS version of these limits, dubbed DURLA, was used in later experiments. As with the changes to the Test Mass 2 sensitive axis position reference changes discussed in the previous section, the use of DURLA did not result in any obvious changes in the time-domain performance of the system, but measurably improved the noise performance in the frequency domain. The use of this mode is also discussed in [4].

Conclusion

The Disturbance Reduction System and the Dynamic Control System met all of their requirements and supported the evaluation of the performance of the Colloidal MicroNewton Thrusters. With only a few exceptions, all control modes performed nominally, with good robustness characteristics. In the few instances where there were problems, the DCS team was able to very quickly provide adjustments to control system parameters to fix them.

Acknowledgements

The authors would like to acknowledge the hard work and dedication of many individuals without whom this mission would not have been possible. Some of these include Jeff D’Agostino and Kathie Blackman of the Hammers Co., who implemented the DCS algorithms into flight software and tested them, as well as supplying simulators to JPL and ESA. Phil Barela, Bill Folkner, Charley Dunn, John Ziemer, Andrew Romero-Wolf, and Mike Girard were just a few of the many engineers at JPL who helped make the mission a success. The DRS mission would not have been possible without the CMNTs developed by Vlad Hruby and the Busek Co. We also received invaluable assistance from engineers at Airbus Defence and Space in Stevenage, UK, and from mission operations personnel at the European Space Operations Centre (ESOC) in Darmstadt, Germany, as we readied our experiment for launch and then throughout commissioning and operations. In particular, we would like to express our gratitude

to Jose Mendes and Ian Harrison of ESOC for their continued support and invaluable insights. Finally, we'd like to thank all of the members of the LISA Pathfinder spacecraft and science teams, especially Project Scientists Paul McNamara and Martin Hewitson and Goddard scientists Ira Thorpe and Jake Slutsky.

References

1. Carmain, A., et. al., "Space Technology 7 Disturbance Reduction System—Precision Control Flight Validation", IEEE Aerospace Conference, Big Sky, MT, USA, March 2005.
2. McNamara, P., et. al., "LISA Pathfinder", Classical Quantum Gravity, 25, 114034 (2008).
3. Hsu, O. C., et. al., "Dynamic Control System Performance During Commissioning of the Space Technology 7 – Disturbance Reduction System Experiment on LISA Pathfinder", AAS 17-155, Proceedings of the AAS GN&C Conference, Breckenridge, CO, February 2017.
4. Maghami, P. G., et. al., "Drag-Free Performance of the ST7 Disturbance Reduction System Flight Experiment on the LISA Pathfinder", 10th International ESA Conference on Guidance, Navigation, and Control Systems, Salzburg, Austria, May-June, 2017.
5. Hruby, V., et. al., "Colloid Thrusters for the New Millennium, ST7 DRS Mission", IEEE Aerospace Conference, Big Sky, MT, USA, March 2004.
6. Maghami, P. G., et. al., "Control Modes of the ST7 Disturbance Reduction System Flight Validation Experiment," SPIE Paper 5528A-17, International Symposium on Optical Science and Technology, Denver, Colorado, USA, August 2004.
7. Hsu, O. C., et. al., "Mode Transitions for the ST7 Disturbance Reduction System Experiment," AIAA Paper 2004-5429, AIAA Guidance, Navigation & Control Conference, Providence, Rhode Island, USA, August 2004.
8. O'Donnell, J. R., et. al., "The Space Technology 7 Disturbance Reduction System—Precision Control Flight Validation," Proceedings of the 19th International Symposium on Space Flight Dynamics, Kanazawa, Japan, June 2006.
9. Maghami, P.G., et. al., "Drag-Free Control Design for the ST7 Disturbance Reduction System Flight Experiment," AIAA paper 2007-6733, AIAA Guidance, Navigation, and Controls Conf., Hilton Head, SC, USA, August 2007.